Chem. Mater. **2006,** *18,* 1029−1035

Magnetic and Transport Properties in Gd$_{1-x}$Sr$_x$CoO$_{3-\delta}$ ($x = 0.10-0.70$)

X. G. Luo, H. Li, X. H. Chen,* Y. M. Xiong, G. Wu, G. Y. Wang, C. H. Wang,
W. J. Miao, and X. Li

*Hefei National Laboratory for Physical Science at Microscale and Department of Physics,
University of Science and Technology of China, Hefei, Anhui 230026, People's Republic of China*

Received September 25, 2005. Revised Manuscript Received December 4, 2005

Magnetic and transport properties of polycrystalline Gd$_{1-x}$Sr$_x$CoO$_{3-\delta}$ ($x = 0.10-0.70$) annealed under the oxygen pressure of 165 atm at 500 °C are systematically investigated. Cluster-glass behavior is observed in the low doping range, while a ferromagnetic transition occurs at the high doping level. Transport measurements indicate insulator-like behavior for the samples with $x \leq 0.30$, an insulator−metal transition around $x = 0.35$, and metallic behavior for higher x samples. However, the large oxygen deficiency leads to a re-entrance of insulator-like state for the samples with $x \geq 0.60$. The annealing procedure under the high oxygen pressure at high temperature can diminish the oxygen deficiency and leads to restoration of the metallic state. The small radius of the Gd^{3+} ion results in less conduction and lower T_c compared to those of La$_{1-x}$Sr$_x$CoO$_3$ and Nd$_{1-x}$Sr$_x$CoO$_3$ as a result of the large structural distortion and the stability of the low-spin state.

I. Introduction

To understand the peculiar electromagnetic properties of the perovskite-type cobalt oxides, Ln$_{1-x}$A$_x$CoO$_3$ (Ln = rare earth element, A = alkli earth metal), such as the large negative magnetoresistance (MR),[1−3] spin- (or cluster-) glass magnetism,[4−7] spin-state transition,[8,9] and insulator−metal (IM) transition induced by doping or temperature,[10,11] numerous works have been performed by many researchers. One important part of these works is to change Ln^{3+} or A^{2+}, to get information of the electronic structure and magnetic states with different ionic radii or hole concentrations.[4,5,12−15]

One striking feature for the richness of the physical properties of Ln$_{1-x}$A$_x$CoO$_3$, compared to other transition oxides such as CMR manganites, nickelates, and cuprates, is the presence of the various spin states for trivalent cobalt ions [low-spin (LS), Co$^{\mathrm{III}}$, t$_{2g}{}^6$e$_g{}^0$; intermediate-spin (IS), Co$^{\mathrm{iii}}$, t$_{2g}{}^5$e$_g{}^1$; high-spin (HS), Co^{3+}, t$_{2g}{}^4$e$_g{}^2$] and tetravalent cobalt ions (LS, Co$^{\mathrm{IV}}$, t$_{2g}{}^5$e$_g{}^0$; IS, Co$^{\mathrm{iv}}$, t$_{2g}{}^4$e$_g{}^1$; HS, Co^{4+}, t$_{2g}{}^3$e$_g{}^2$) and the relative narrow energy gap between these spin states. This makes a thermal spin-state transition occur easily.[5,16] Recent experimental and theoretical investigations indicate that the spin states are LS and a mixture of IS/LS for tetravalent and trivalent cobalt ions, respectively.[9,12,17−22] The conversion of different spin states arises from the competition between the comparable magnitudes of the crystal field with energy Δ_{CF} (t$_{2g}$−e$_g$ splitting) and the intraatomic (Hund) exchange with energy J_{ex}, leading to the redistribution of electrons between the t$_{2g}$ and the e$_g$ levels. Δ_{CF} is found to be very sensitive to the variation in the Co−O bond length ($d_{\mathrm{Co-O}}$), so the subtle balance between Δ_{CF} and J_{ex} may be easily disrupted by different kinds of effects, such as the hole-doping and the chemical/external pressure.[23−26] Among

---

* Corresponding author. E-mail: chenxh@ustc.edu.cn.

(1) Brinceno, G.; Chang, H.; Sun, X.; Shulz, P. G.; Xiang, X. D. *Science* **1995**, *270*, 273.
(2) Golovanov, V.; Mihaly, L.; Moodenbuagh, A. R. *Phys. Rev. B* **1996**, *53*, 8207.
(3) Mahendiram, R.; Raychaudhuri, K. *Phys. Rev. B* **1996**, *54*, 16044.
(4) Itoh, M.; Natori, I.; Kubota, S.; Motoya, K. *J. Phys. Soc. Jpn.* **1994**, *63*, 1486.
(5) Senaris-Rodriguez, M. A.; Goodenough, J. B. *J. Solid State Chem.* **1995**, *118*, 323.
(6) Mukherjee, S.; Ranganathan, R.; Anilkumar, P. S.; Joy, P. A. *Phys. Rev. B* **1996**, *54*, 9267.
(7) Anilkumar, P. S.; Joy, P. A.; Date, S. K. *J. Phys.: Condens. Matter* **1998**, *10*, L487.
(8) Mukherjee, S.; Raychaudhuri, P.; Nigam, A. K. *Phys. Rev. B* **2000**, *61*, 8651.
(9) Loshkareva, N. N.; Gan'shina, E. A.; Belevtsev, B. I.; Sukhorukov, Y. P.; Mostovshchikova, E. V.; Vinogradov, A. N.; Krasovitsky, V. B.; Chukanova, I. N. *Phys. Rev. B* **2003**, *68*, 024413.
(10) Tsubouchi, S.; Kyomen, T.; Itoh, M.; Ganguly, P.; Oguni, M.; Shimojo, Y.; Morii, Y.; Ishii, Y. **2002**, *66*, 052418.
(11) Moritomo, Y.; Takeo, M.; Liu, X. J.; Akimoto, T.; Nakamura, A. *Phys. Rev. B* **1998**, *58*, R13334.
(12) Saitoh, T.; Mizokawa, T.; Fujimori, A.; Abbate, M.; Takeda, Y.; Takano, M. *Phys. Rev. B* **1997**, *56*, 1290. Saitoh, T.; Mizokawa, T.; Fujimori, A.; Abbate, M.; Takeda, Y.; Takano, M. *Phys. Rev. B* **1997**, *55*, 4257.
(13) Sehlin, S. R.; Anderson, H. U.; Sparlin, S. M. *Phys. Rev. B* **1995**, *52*, 11681.
(14) Ganguly, R.; Hervieu, M.; Nguyen, N.; Maignan, A.; Martin, C.; Raveau, B. *J. Phys.: Condens. Matter* **2001**, *13*, 10911.
(15) Yoshii, K.; Abe, H.; Nakamura, A. *Mater. Res. Bull.* **2001**, *36*, 1447.
(16) Raccah, P. M.; Goodenough, J. B. *Phys. Rev.* **1967**, *155*, 932.
(17) Korotin, M. A.; Ezhov, S. Y.; Solovyev, I. V.; Anisimov, V. I.; Khomskii, D. I.; Sawatzky, G. A. *Phys. Rev. B* **1996**, *54*, 5309.
(18) Yamaguchi, S.; Okimoto, Y.; Tokura, Y. *Phys. Rev. B* **1997**, *55*, 8666.
(19) Louca, D.; Sarrao, J. L.; Thompson, J. D.; Roder, H.; Kwei, G. H. *Phys. Rev. B* **1999**, *60*, R10378.
(20) Kobayashi, Y.; Fujiwara, N.; Murata, S.; Asai, K.; Yasuoka, H. *Phys. Rev. B* **2000**, *62*, 410.
(21) Zobel, C.; Kriener, M.; Bruns, D.; Baier, J.; Gruninger, M.; Lorenz, T.; Reutler, P.; Revcolevschi, A. *Phys. Rev. B* **2002**, *66*, 020402.
(22) Ravindran, P.; Fjellvag, H.; Kjekshus, A.; Blaha, P.; Schwarz, K.; Luitz, J. *J. Appl. Phys.* **2002**, *91*, 291.
(23) Asai, K.; Yokokura, O.; Suzuki, M.; Naka, T.; Matsumoto, T.; Takahashi, H.; Mori, N.; Kohn, K. *J. Phys. Soc. Jpn.* **1997**, *66*, 967. Asai, K.; Yoneda, A.; Yokokura, O.; Tranquada, J. M.; Shirane, G.; Kohn, K. *J. Phys. Soc. Jpn.* **1998**, *67*, 290.

10.1021/cm0521471 CCC: \$33.50

them, chemical pressure on CoO_6 octahedra is usually generated by decreasing the average Ln-site ionic radius $\langle r \rangle$, which can cause the insulating nonmagnetic LS state because of the increase of the Δ_{CF} with the reduction of the CoO_6 octahedra volume, which results in the depopulation of the magnetic e_g level.

Another pronounced feature in perovskite cobaltites is that the ferromagnetic (FM) state evolves as a result of increasing hole doping level in low x, in the paramagnetic matrix with dominant antiferromagnetic (AFM) superexchange interactions between Co^{3+} ions through a spin- or cluster-glass-state region.[27,28] The competition between FM and AFM interactions leads to a highly inhomogeneous ground state exhibiting the coexistence of FM regions, spin-glass (SG) regions, and hole-poor LS regions.[9,29−31] The evolution of these regions and the spin states with hole concentration leads to the intricate magnetic and electronic behaviors. Studies on the $La_{1-x}Sr_xCoO_3$ system (La(Sr) compounds) reveal a rather rich magnetic and electronic phase diagram with the doping level: SG for $x < 0.18$, cluster FM behaviors for $x \geq 0.18$, insulator-like/metallic resistivity, IM transition at $x \approx 0.20$, and so on.[4,27] Ca- and Ba-doped compounds $La_{1-x}A_xCoO_3$ (A = Ca and Ba) have also been studied intensively.[32,33]

Besides the La compounds, other important perovskite cobaltites such as $Ln_{1-x}Sr_xCoO_3$ ($Ln^{3+} = Pr^{3+}$, Nd^{3+}, Sm^{3+}, Eu^{3+}, Gd^{3+}, etc.) also exhibit complex magnetic and electrical properties.[32−39] In this paper, we investigated Sr-doped gadolinium cobaltites systematically. However, most of the work on $Gd_{1-x}Sr_xCoO_{3-\delta}$ (Gd(Sr) compounds) was focused on the evolution of crystal structure with Sr doping[38,40] and magnetic and transport properties at relatively high temperature ($T > 77$ K).[38,40] The Gd^{3+} ion has characters different from those of the La^{3+} ion, for example, an ionic radius smaller than that of the La^{3+} ion and a high magnetic moment with no $L-S$ anisotropy ($L = 0$, $S = 7/2$),[41] in contrast to the nonmagnetic La^{3+} ($L = 0$, $S = 0$). Therefore, behavior contrasting that of La(Sr) compounds should be expected in Gd(Sr) compounds. In fact, some distinct properties from La(Sr) compounds have been reported in the Gd(Sr) compounds. In undoped sample $GdCoO_3$, the cobalt ions are in a LS state below 270 K,[42] while in $LaCoO_3$, the mixture of the LS/IS state is observed above about 100 K.[43−45] Specifically, no metallic behavior is reported in the $Gd_{1-x}Sr_xCoO_{3-\delta}$ system below 300 K so far,[38,40,41] in contrast to the metallic resistivity for $x > 0.20$ in La(Sr) compounds. In this paper, samples annealed under the oxygen pressure of 165 atm at 500 °C are systematically investigated. Cluster-glass behavior is found in the low doping range, while a FM transition is observed at a high doping level. Transport measurements indicate insulator-like behavior for the samples with $x \leq 0.30$, an IM transition around $x = 0.35$, and metallic behavior for the samples with higher x. The system re-enters the insulator-like state for $x \geq 0.60$, resulting from the existence of large oxygen deficiency, and the metallic state can be restored by annealing the samples at 900 °C under the high oxygen pressure of 240 atm. We found that the Gd(Sr) compounds possess less conductance and a lower FM transition temperature relative to La(Sr) compounds[27] and $Nd_{1-x}Sr_xCoO_3$ (Nd(Sr) compounds),[37] which is attributed to the large structural distortion and the stability of the LS state arising from the smaller radius of the Gd^{3+} ion.

II. Experiment

Polycrystalline $Gd_{1-x}Sr_xCoO_{3-\delta}$ ($x = 0.10-0.70$) samples were prepared through conventional solid-state reaction. The stoichiometric amounts of Gd_2O_3, $SrCO_3$, and Co_3O_4 powders were thoroughly mixed and fired at 1200 °C. After that, the mixture was reground and pressed into pellets which were sintered at 1200 °C for 24 h. This procedure was repeated three times. To get the homogeneous sample with less oxygen deficiency, the samples were then annealed under the oxygen pressure of 165 atm at 500 °C for 48 h. X-ray diffraction (XRD) was performed by a Rigaku D/max-A X-ray diffractometer with graphite monochromated Cu Kα radiation ($\lambda = 1.5418$ Å) at room temperature. Magnetization measurement was carried out with a superconducting quantum interference device (SQUID) magnetometer (MPMS-7XL, Quantum Design). The resistivity measurements were performed by using the standard alternating current (ac) four-probe method. The magnetic field was supplied by a superconducting magnet system (Oxford Instruments). We also determined the oxygen content of the samples using the $K_2Cr_2O_7$ titration method. An appropriate amount of sample (about 30 mg) was dissolved in the mixture of vitriol and phosphate acid, then the high valent Co ions were deoxidized to divalent ones with

---

(24) Lengsdorf, R.; Ait-Tahar, M.; Saxena, S. S.; Ellerby, M.; Khomskii, D. I.; Micklitz, H.; Lorenz, T.; Abd-Elmeguid, M. M. *Phys. Rev. B* **2004**, *69*, 140403.

(25) Vogt, T.; Hriljac, J. A.; Hyatt, N. C.; Woodward, P. *Phys. Rev. B* **2003**, *67*, 140401.

(26) Fita, I.; Szymczak, R.; Puzniak, R.; Troyanchuk, I. O.; Fink-Finowicki, J.; Mukovskii, Y. M.; Varyukhin, V. N.; Szymczak, H. *Phys. Rev. B* **2005**, *71*, 214404.

(27) Wu, J.; Leighton, C. *Phys. Rev. B* **2003**, *67*, 174408.

(28) Nam, D. N. H.; Jonason, K.; Nordblad, P.; Khiem, N. V.; Phuc, N. X. *Phys. Rev. B* **1999**, *59*, 4189.

(29) Kuhns, P. L.; Hoch, M. J. R.; Moulton, W. G.; Reyes, A. P.; Wu, J.; Leighton, C. *Phys. Rev. Lett.* **2003**, *91*, 127202.

(30) Hoch, M. J. R.; Kuhns, P. L.; Moulton, W. G.; Reyes, A. P.; Lu, J.; Wu, J.; Leighton, C. *Phys. Rev. B* **2004**, *70*, 174443.

(31) Ghoshray, A.; Bandyopadhyay, B.; Ghoshray, K.; Morchshakov, V.; Bärner, K.; Troyanchuk, I. O.; Nakamura, H.; Kohara, T.; Liu, G. Y.; Rao, G. H. *Phys. Rev. B* **2004**, *69*, 064424.

(32) Rao, C. N. R.; Parkash, O. M.; Bahadur, D.; Ganguly, P.; Share, A. N. *J. Solid State Chem.* **1977**, *22*, 353.

(33) Kriener, M.; Zobel, C.; Reichl, A.; Baier, J.; Cwik, M.; Berggold, K.; Kierspel, H.; Zabara, O.; Freimuth, A.; Lorenz, T. *Phys. Rev. B* **2004**, *69*, 094417.

(34) Brinks, H. W.; Fjellvåg, H.; Kjekshus, A.; Hauback, B. C. *J. Solid State Chem.* **1999**, *147*, 464.

(35) Fondado, A.; Breijo, M. P.; Rey-Cabezudo, C.; Sanchez-Andujar, M.; Mira, J.; Rivas, J.; Senaris-Rodriguez, M. A. *J. Alloys Compd.* **2001**, *323−324*, 447.

(36) Senaris-Rodriguez, M. A.; Breijo, M. P.; Castro, S.; Rey, C.; Sanche, M.; Sanchez, R. D.; Mira, J.; Fondado, A.; Rivas, J. *Int. J. Inorg. Mater.* **1999**, *1*, 281.

(37) Stauffer, D. D.; Leighton, C. *Phys. Rev. B* **2004**, *70*, 214414.

(38) Ryu, K. H.; Sun, K. S.; Lee, S. J.; Yo, C. H. *J. Solid State Chem.* **1993**, *105*, 550.

(39) Krimmel, A.; Reehuisl, M.; Paraskevopoulos, M.; Hemberger, J.; Loidl, A. *Phys. Rev. B* **2001**, *64*, 224404.

(40) Takeda, Y.; Ueno, H.; Imanishi, N.; Yamamoto, O.; Sammes, N.; Phillipps, M. B. *Solid State Ions* **1996**, *86−88*, 1187.

(41) Rey-Cabezudo, C.; Sanchez-Andujar, M.; Mira, J.; Fondado, A.; Rivas, J.; Senaris-Rodriguez, M. A. *Chem. Mater.* **2002**, *14*, 493.

(42) Casalot, A.; Dougier, P.; Hagenmuller, P. *J. Phys. Chem. Solids* **1971**, *32*, 407.

(43) Sudheendra, L.; Seikh, M. M.; Raju, A. R.; Narayana, C. *Chem. Phys. Lett.* **2001**, *340*, 275.

(44) Chang, J. Y.; Lin, B. N.; Hsu, Y. Y.; Ku, H. C. *Physica B* **2003**, *329*, 826.

(45) Knizek, K.; Jirak, Z.; Hejtmanek, J.; Veverka, M.; Marysko, M.; Maris, G.; Palstra, T. T. M.; cond-mat/0503104 2005.

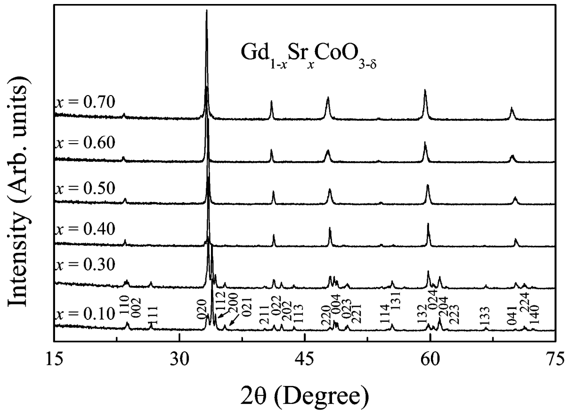

Figure 1. X-ray powder diffraction patterns for $Gd_{1-x}Sr_xCoO_{3-\delta}$ ($0.10 \le x \le 0.70$).

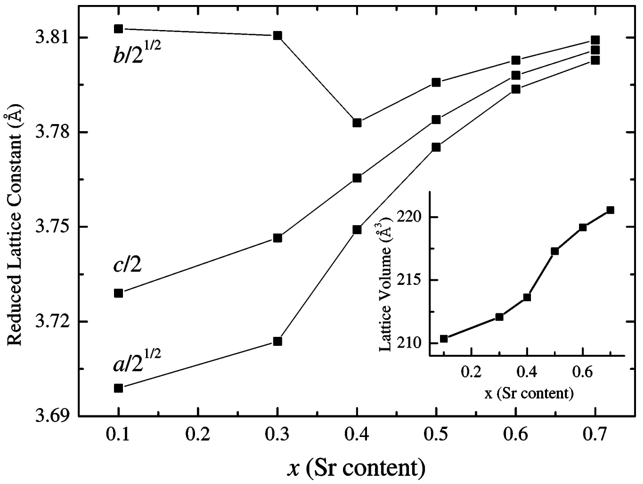

Figure 2. Reduced lattice constants vs Sr content (x) in $Gd_{1-x}Sr_xCoO_{3-\delta}$ ($0.10 \le x \le 0.70$). Inset: The variation of the lattice volume with Sr content (x).

Fe^{2+} ions, and finally the excess Fe^{2+} ions were titrated with $K_2Cr_2O_7$ solution.

III. Experimental Results

A. XRD Patterns. Figure 1 shows the XRD patterns for $Gd_{1-x}Sr_xCoO_{3-\delta}$ ($x = 0.10-0.70$). The XRD patterns indicate that the obtained samples were all single phase and exhibited an O-type orthorhombic $GdFeO_3$-like distorted perovskite structure (SG, *Pnma*, $a_{ort}/\sqrt{2} \le c_{ort}/2 \le b_{ort}\sqrt{2}$), which has been used in $GdCoO_3$[42] and $Gd_{0.5}Sr_{0.5}CoO_3$.[46] The variation of lattice parameters with x was plotted in Figure 2. The lattice parameters a and c increase monotonically with the doping level, while b first decreases with $x < 0.4$ and then increases with further increasing x. It is found that the difference among the reduced parameters becomes less with increasing x and is nearly the same for $x = 0.7$, indicative of a tendency of cubic symmetry. This is reasonable because $SrCoO_3$ is cubic.[47] The lattice volume, shown in the inset of Figure 2, increases monotonically with x, which is consistent with the substitution of the larger Sr^{2+} ions (${}^{XII}r_{Sr^{2+}} = 1.58$ Å) for the smaller Gd^{3+} ions (${}^{XII}r_{Gd^{3+}} = 1.22$ Å).[48,49]

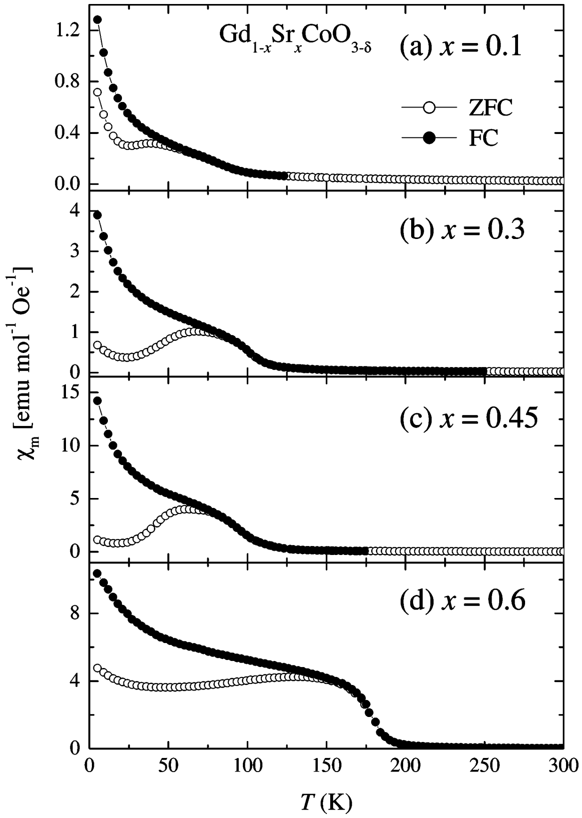

Figure 3. ZFC and FC molar magnetic susceptibility of $Gd_{1-x}Sr_xCoO_{3-\delta}$ ($x = 0.10$, 0.30, 0.45, and 0.60) as a function of temperature at $H = 1000$ Oe.

B. Magnetic Properties. Figure 3 shows the molar magnetic susceptibility $\chi_m(T)$ as a function of temperature in zero-field-cooled (ZFC) and field-cooled (FC) procedures for the four typical samples. For the sample with $x = 0.60$, the $\chi_m(T)$ curve behaves as a typical ferromagnet so that a pronounced increase in $\chi_m(T)$ occurs below a temperature T_c (≈180 K), with a paramagnetic signal at low temperature, which comes from the contribution of magnetic Gd^{3+} ions. The T_c corresponds to the FM transition temperature. With decreasing Sr concentration, the rise begins to slow and T_c decreases sharply (from about 120 K for $x = 0.45$ to 80 K for $x = 0.10$). A rounded maximum appears below T_c in the ZFC $\chi_m(T)$ curves. This behavior may be ascribed to the SG magnetism, which has been reported in La(Sr) and Nd(Sr) compounds with a low doping level.[5,27,37] In La(Sr) and Nd(Sr) compounds, the ZFC curve shows a cusp at the freezing temperature of SG.[5,27,37] However, the ZFC and FC curves in the two compounds bifurcate at a temperature much higher than that of the cusp,[5,27,37] in contrast to the behavior observed in present Gd(Sr) compounds. Therefore, one may assume that Gd(Sr) compounds have magnetic property different from those of the La(Sr) and Nd(Sr) systems in the low doping region. To clarify this, the frequency dependence of ac susceptibility was measured. Figure 4a,b shows the temperature dependence of $\chi_m'(T)$ and $\chi_m''(T)$ (the in-phase and out-of-phase component of the ZFC ac susceptibility) for the sample with $x = 0.10$ taken at 10 and 1000 Hz. A peak can be observed in both $\chi_m'(T)$ and $\chi_m''(T)$

---

(46) Vanitha, P. V.; Arulraj, A.; Santhosh, P. N.; Rao, C. N. R. *Mater. Chem.* **2002**, *12*, 1666.
(47) Shaplygin, I.; Lazarev, V. *Russ. J. Inorg. Chem.* **1985**, *30*, 1828.
(48) Shannon, R. D. *Acta Crystallogr., Sect. A* **1976**, *32*, 751.
(49) Shannon, R. D.; Prewitt, C. T. *Acta Crystallogr., Sect. B* **1969**, *25*, 925.

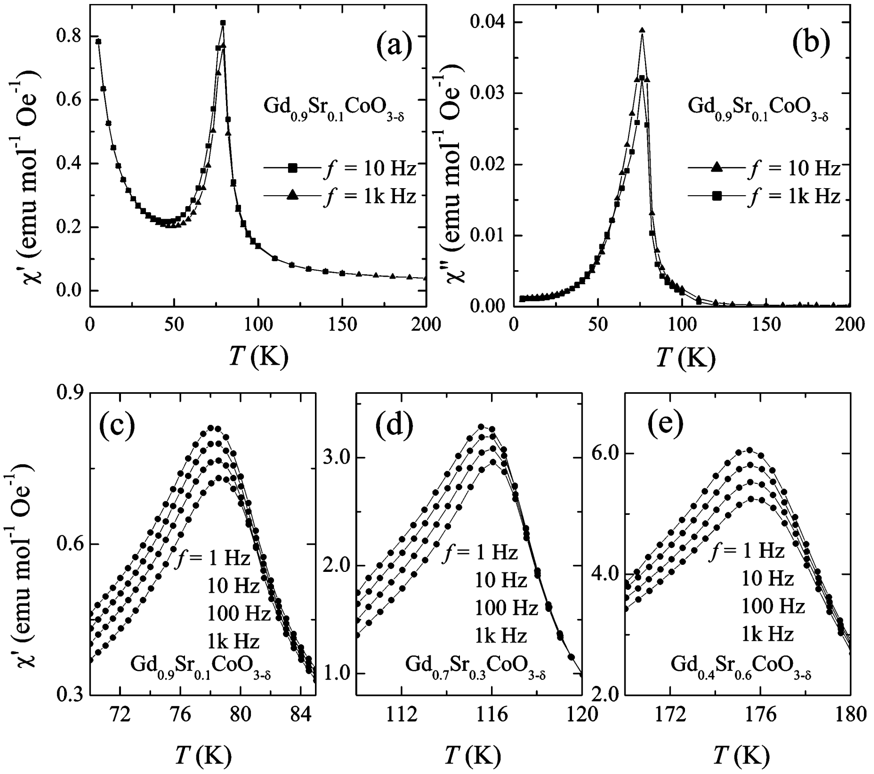

Figure 4. (a, b) Temperature dependence of the in-phase and out-of-phase components of the ac susceptibility for $x = 0.10$. The data were taken at 10 and 1000 Hz as indicated in the figure. (c−e) Closeup of the temperature dependence of the in-phase ac susceptibility at the four frequencies in the range 1−1000 Hz for the samples with $x = 0.10$, 0.30, and 0.60, respectively.

at 75 K. In La(Sr) and Nd(Sr) compounds, the temperature corresponding to the peak $\chi_m'(T)$ is the same as that of cusp in ZFC direct current (dc) susceptibility.[27,37] However, this temperature is much higher by 30 K than that corresponding to the maximum of the ZFC $\chi_m(T)$ in $Gd_{0.9}Sr_{0.1}CoO_{3-\delta}$. It is well-known that the peak temperature in ac susceptibility for a SG should be the same as that in ZFC susceptibility, which represents a magnetic freezing temperature of SG. Thus, the ac susceptibility data exclude the possibility of the existence of a SG in Gd(Sr) compounds with low doping. The absence of the SG for $x = 0.10$ is illustrated more clearly by the near frequency independence of the peak temperature of $\chi_m'(T)$ in Figure 4c, which shows a "closeup" of this peak in $\chi_m'(T)$, measured with a temperature spacing of 0.5 K. Measured from 1 to 1000 Hz, the peak temperature of $\chi_m'(T)$ shifts to the higher side by less than 0.65% (= 0.5 K/77 K), while it is much larger than this value in La(Sr) and Nd(Sr) compounds (for instance, it changes about 2% in La(Sr) compounds).[27,37] Consequently, the peak in ac susceptibility could not be an indication of a SG behavior. Figure 4d,e also displays the "closeup" of the ac susceptibility $\chi_m'(T)$ for the samples with $x = 0.30$ and 0.60. With the frequency changing from 1 to 1000 Hz, the peak of $\chi_m'(T)$ for $x = 0.30$ shifts to higher temperature by less than 0.5 K, while the peak position for $x = 0.60$ is independent of the frequency. From Figure 3a,b, it can be concluded that there is a small FM component in the samples with $x = 0.10$ and 0.30. Apparently, FM clusters are very diluted by a nonmagnetic matrix in this compound and interact very weakly with each other. Therefore, the weak frequency dependence of the temperature corresponding to the peak of $\chi_m'(T)$ in the samples with $x = 0.10$ and 0.30 suggests existence of a cluster-glass, while the frequency independence of the peak position for the sample with $x = 0.60$ indicates a FM transition.

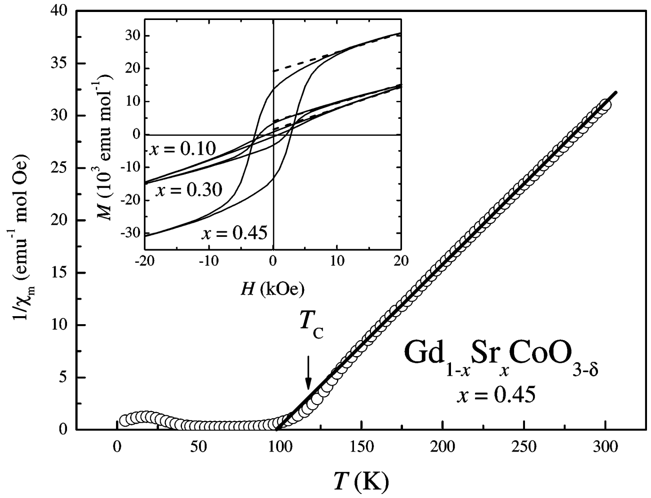

Figure 5. Inverse ZFC molar magnetic susceptibility as a function of temperature for the sample with $x = 0.45$. The solid line is the fitting curve according to the Curie−Weiss law for the high-temperature data. The inset shows the $M-H$ loop for the samples with $x = 0.10$, 0.30, and 0.45 at 5 K between −2 T to 2 T. The dashed lines in the inset extrapolate the $M(H)$ to $H = 0$ to determine the spontaneous magnetization.

Figure 5 shows the ZFC $1/\chi_m(T)$ as a function of T for the sample with $x = 0.45$. The $\chi_m(T)$ can be well fitted with the Curie−Weiss law in the temperature range above T_c. On the basis of the fitting result, the effective magnetic moment per cobalt ions μ_{eff-Co} can be obtained by subtracting the Gd^{3+} contribution ($\mu_{eff}(Gd^{3+}) = 7.94\ \mu_B$) from the total $\mu_{eff} = \sqrt{(8C)}$ (C, the Curie constant).[50] The obtained μ_{eff-Co} is 2.96 μ_B, which is much less than 3.67 μ_B in $La_{1-x}Sr_xCoO_3$

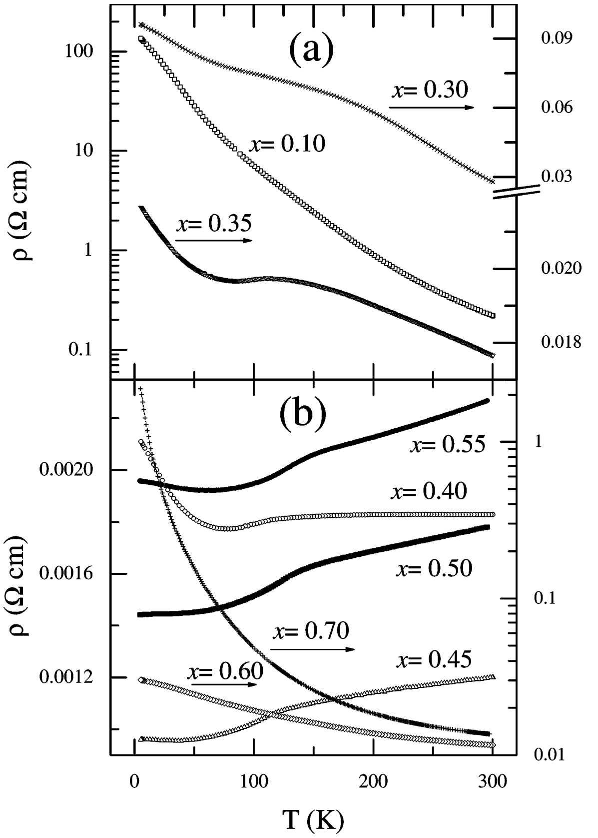

Figure 6. Temperature dependence of resistivity for $Gd_{1-x}Sr_xCoO_{3-\delta}$ ($0.10 \leq x \leq 0.70$).

with the same doping level,[5] indicative of a lower spin state for Gd(Sr) compounds relative to La(Sr) compounds. The inset of Figure 5 shows the $M(H)$ loop for the sample with $x = 0.45$ at 5 K, exhibiting FM behavior with spontaneous magnetization and clear hysteresis with a paramagnetic component. The nonsaturating component comes from the corporate effect of large paramagnetic signal from Gd^{3+} ions and the cluster nature of the FM state,[9,29−31] where some fraction of the Co spins exists in the paramagnetic matrix. It should be pointed out that the coercive field for this sample at 5 K is as large as 2850 Oe, which is much larger than that in La(Sr) compounds[5,27] but comparable to that in Nd(Sr) compounds.[37] This pronounced coercive behavior is believed to reflect the magnetic inhomogeneity and the formation of FM clusters.[9,29−31] We note that in the inset of Figure 5 the samples with $x = 0.10$ and 0.30 also show a small spontaneous magnetization, which can be comparable with that observed in low doping La(Sr) compounds.[5,27] Such a small spontaneous magnetization at 5 K and the weak frequency dependence of the temperature corresponding to the peak in $\chi_m'(T)$ for the two samples indicate a cluster-glass. Actually, Rey-Cabezudo et al.[41] have considered a cluster picture about the magnetism for the Gd(Sr) samples with $x \leq 0.30$.

C. Transport Properties. Figure 6 shows the temperature dependence of resistivity $\rho(T)$ for the $Gd_{1-x}Sr_xCoO_{3-\delta}$ system ($0.10 \leq x \leq 0.70$). The $x = 0.10$ sample exhibits an insulating behavior in the whole temperature range. With increasing Sr content up to 0.45, $\rho(T)$ decreases dramatically. At 4.2 K, $\rho(T)$ drops by more than 1000 times for the sample with $x = 0.30$ and by more than 10^5 times for the sample with $x = 0.45$ relative to the sample with $x = 0.10$. An IM transition occurs around 110 K as the Sr content increases up to 0.35. The sample with $x = 0.45$ shows metallic behavior down to 4.2 K and a kink around 120 K, which coincides with the FM transition temperature. Such a kink in $\rho(T)$ is a common feature for an itinerant ferromagnet because of the reduction of scattering from spin disorder in the FM state as observed in CMR manganites[51] and $La_{1-x}Sr_xCoO_3$ ($0.30 \leq x \leq 0.60$).[5] With further increasing Sr content above 0.45, the $\rho(T)$ increases rapidly. The $\rho(T)$ for the sample with $x = 0.50$ shows still metallic behavior in whole temperature range, while an upturn in low temperature is observed in $\rho(T)$ for the sample with $x = 0.55$. It should be pointed out that the position of the kink in $\rho(T)$ shifts to higher temperature with increasing x from 0.40 to 0.55, which is consistent with the enhancement of T_c with increasing x as shown in Figure 3. As the Sr content increases to 0.60, the resistivity shows a re-entrance of the insulating state.

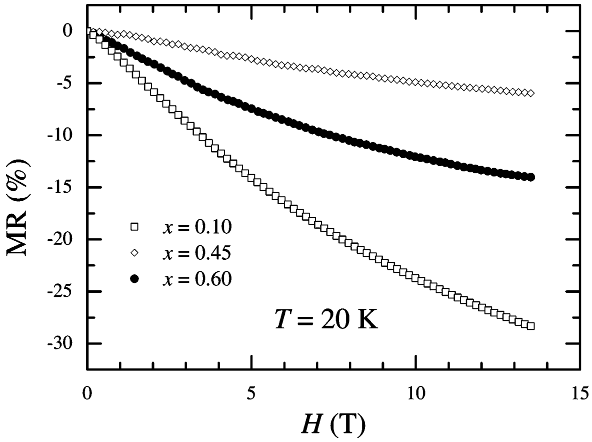

Figure 7. Isothermal MR ($T = 20$ K) as a function of magnetic field for the samples with $x = 0.10$, 0.45, and 0.60, respectively.

Figure 7 shows the isothermal MR at 20 K as a function of magnetic field for $Gd_{1-x}Sr_xCoO_{3-\delta}$ with $x = 0.10$, 0.45, and 0.60, respectively. A large negative MR $[(\rho(0) - \rho(H))/\rho(0)] \times 100\%$ as high as -28.5% is achieved in the sample with $x = 0.10$ at 13.5 T. In the sample with $x = 0.45$, which is the most metallic among all the samples, exhibits a smallest negative MR $\approx -6\%$ at 13.5 T. The MR in the sample with $x = 0.60$ increases to -14% at 13.5 T. This suggests that magnetic field has the strongest effect on the most insulating samples. It suggests that the MR depends on not only the FM state but also the insulating state.

Attention should be paid to the insulator-re-entering behavior for $x \geq 0.60$ because the end compound $SrCoO_3$ is metallic. To consider the origin for the re-entrance of the insulating state, one must note the fact that it is difficult to achieve full oxygen stoichiometry at a high-doping level in the $Ln_{1-x}Sr_xCoO_3$ system. Yo et al.[52] found that there exists large oxygen deficiency in $Dy_{1-x}Sr_xCoO_{3-\delta}$ and $Sm_{1-x}Sr_x$-

---

(50) Dekker, A. *Solid State Physics*; Prentice-Hall: New York, 1970; p 450.

(51) *Colossal Magnetoresistive Oxides*; Tokura, Y., Ed.; Gordan and Breach: Amsterdam, 2000.

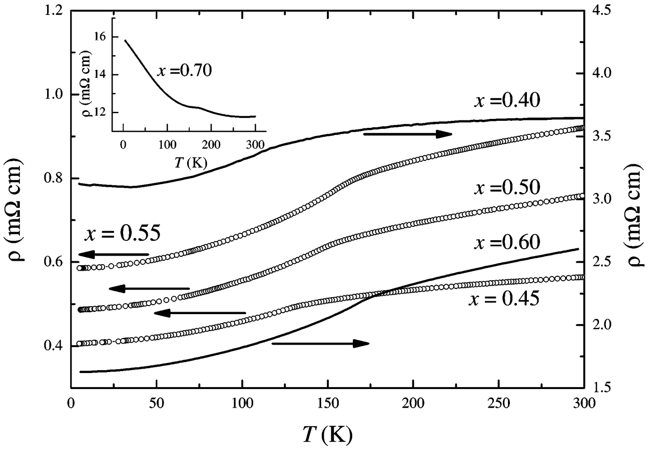

Figure 8. Temperature dependence of the resistivity for the samples with $x = 0.40-0.70$ after annealing under the high oxygen pressure of 240 atm at 900 °C for 48 h.

$CoO_{3-\delta}$, and the oxygen deficiency reaches 0.29 and 0.36 for the samples with $x = 0.75$ for the two systems, respectively. Ryu et al.[38] reported that there also exists large oxygen deficiency in $Gd_{1-x}Sr_xCoO_{3-\delta}$ for the samples with high doping level. Therefore, to understand the re-entrance of the insulator state, the oxygen content is determined. The $K_2Cr_2O_7$ titration experiments indicate that the oxygen contents are 2.912, 2.728, and 2.602 for as-grown samples with $x = 0.45$, 0.60, and 0.70, respectively, while they are 2.935, 2.745, and 2.703 after annealing under the oxygen pressure of 165 atm at 500 °C for 48 h. It turns out that there really exists a large oxygen deficiency at a high doping level, and an annealing procedure under high oxygen pressure reduces the deficiency. Compared to the annealing procedure at 500 °C, the samples are annealed under the high oxygen pressure of 240 atm at 900 °C, and the resistivity for these samples is shown in Figure 8. The sample with $x = 0.60$ exhibits metallic resistivity in the whole temperature range below 300 K. The sample with $x = 0.70$ also becomes much less insulating, with $\rho(T = 5\ \text{K})/\rho(T = 300\ \text{K}) < 4/3$, in contrast to that annealed at 500 °C (larger than 100). The metallic state should be restored in the sample with $x = 0.70$ after further annealing under higher oxygen pressure. The $K_2Cr_2O_7$ titration experiments indicate that the oxygen contents are 2.787 and 2.755 for $x = 0.60$ and 0.70 after annealing under the oxygen pressure of 240 atm at 900 °C, respectively. It is clear that the oxygen deficiency leads to the re-entrance of the insulating behavior for the samples with $x \geq 0.60$.

IV. Discussion

Figure 9 shows the phase diagram of $Gd_{1-x}Sr_xCoO_{3-\delta}$ ($0.10 \leq x \leq 0.70$) according to the above results. In Figure 9, one can find a pronounced feature that the $Gd_{1-x}Sr_xCoO_{3-\delta}$ system has a much lower FM transition temperature compared to La(Sr) and Nd(Sr) compounds, for instance, T_c in $Gd_{0.5}Sr_{0.5}CoO_{3-\delta}$ annealed under the high oxygen pressure of 240 atm at 900 °C ($\delta \approx 0.032$) is around 150 K, while in $La_{0.5}Sr_{0.5}CoO_3$ it is about 240 K. Another feature in Figure 9 is that the critical Sr concentration for IM transition (≈0.35) is much larger than that in La(Sr) and Nd(Sr) compounds. Taking into account the fact that the less conducting $Gd_{1-x}Sr_xCoO_{3-\delta}$ samples have the lower T_c, one may suppose a correlation between metallic conductivity and FM order as it would be expected with a double-exchange model as in doped manganites. This opinion could be supported by the fact that both the conductance and T_c increases as oxygen content increases, as inferred from Figures 6, 8, and 9. It is well-known that T_c in doped manganites is argued to be mainly determined by two kinds of structural distortion.[53] This is also believed to be plausible in cobaltites.[33,46] The first is a global distortion arising from the deviation of the structure from the cubic symmetry, which is described by the deviation of the tolerant factor t [$= (\langle r_A\rangle + r_O)/\sqrt{2}(r_{Co} + r_O)$ for the formation of $ACoO_3$]. The much smaller ion radius of the Gd^{3+} ion relative to La^{3+} (${}^{XII}r_{La}{}^{3+} = 1.36$ Å) or Nd^{3+} (${}^{XII}r_{Nd}{}^{3+} = 1.30$ Å) ions[48,49] leads to a much smaller tolerant factor in Gd(Sr) compounds compared to those in La(Sr) and Nd(Sr) compounds. The second is a local distortion arising from the different ion radii at the A site, which is described by the variance of the A-site ionic radii σ^2 [$= (1 - x)r_{Ln}{}^2 + xr_M{}^2 - \langle r_A\rangle$ for $Ln_{1-x}M_xCoO_3$, where $\langle r_A\rangle = (1 - x)r_{Ln} + xr_M$]. The radius of the Sr^{2+} ion is much larger than that of the Gd^{3+} ion, which results in a large local distortion (such as, when $Ln_{0.5}Sr_{0.5}CoO_3$, $\sigma^2 = 0.0123$ for Ln = Gd, while $\sigma^2 = 0.0016$ for Ln = La, and $\sigma^2 = 0.0072$ for Ln = Nd).[46] Consequently, the small tolerant factor in $Gd_{1-x}Sr_xCoO_{3-\delta}$ samples means a large deviation from cubic symmetry, and the large σ^2 suggests a pronounced local disorder. They lead to a dramatic reduction in the FM exchange and, thus, the FM transition temperature and conductance. In addition, $Gd_{1-x}Sr_xCoO_{3-\delta}$ is a more complex

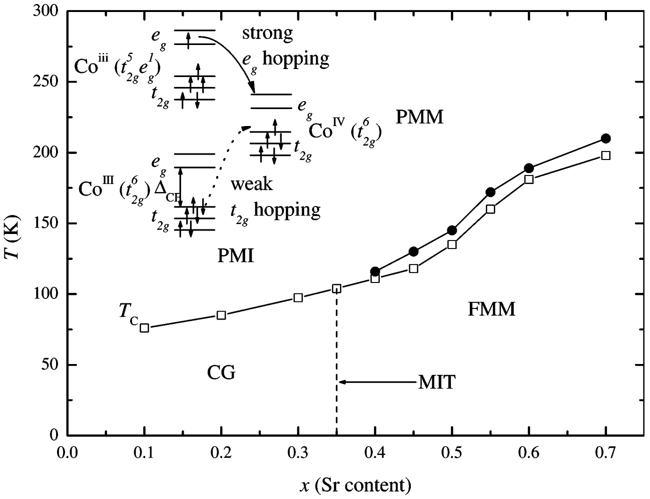

Figure 9. Schematic drawing of the $T-x$ phase diagram for the $Gd_{1-x}Sr_xCoO_{3-\delta}$ ($0.10 \leq x \leq 0.70$) system. T_c: determined from both the dc susceptibility and the ac susceptibility (□, the samples annealed under the oxygen pressure of 165 atm at 500 °C; ●, the samples annealed under the oxygen pressure of 240 atm at 900 °C); CG, cluster-glass; FMM, ferromagnetic metal; PMI/PMM, paramagnetic insulator/metal; MIT, insulator−metal transition. Inset: possible hopping procedure between trivalent cobalt ions and Co^{IV}. Δ_{CF}: the energy of crystal field splitting.

---

(52) Kang, J. W.; Ryu, K. H.; Yo, C. H. *Bull. Korean Chem. Soc.* **1995**, *16*, 600. Jeong, S. K.; Kim, M. G.; Kim, K. H.; Yo, C. H. *Bull. Korean Chem. Soc.* **1996**, *17*, 794.

(53) Rodriguez-Martinez, L. M.; Attifield, J. P. *Phys. Rev. B* **1996**, *54*, R15622.

system because of the large oxygen deficiency at high doping level, which would influence the structural distortion and the carrier concentration markedly. This could be another cause for the low FM transition temperature and conductance.

Actually, there is a further reason for the suppression of conductance and ferromagnetism in $Gd_{1-x}Sr_xCoO_{3-\delta}$. Compared to manganites, the conversion of various spin-states of Co ions in cobaltites seriously influences the magnetic and the transport properties of cobaltites. The FM exchange and charge transport are thought to occur mainly through the hopping of e_g electrons, as shown in the inset of Figure 9. The t_{2g} electron hopping can also occur, but it has a much smaller possibility of taking place. Therefore, the existence of e_g electrons is vital for metallic FM order. Recently, Lengsdorf et al.[24] reported a transition from the conducting state to the insulating state and a decrease of T_c induced by pressure in $La_{0.82}Sr_{0.18}CoO_3$. This peculiar behavior has been attributed to a gradual change of the spin state for the trivalent ions from a magnetic to a nonmagnetic spin state under pressure. In $LaCoO_3$, it was found to undergo an intermediate- to low-spin-state transition under pressure.[25] The change of the spin state with pressure is realized because of the increase in the energy of the crystal-field splitting (Δ_{CF}) under pressure. The increase of Δ_{CF} makes the LS Co^{III} more stable. The Gd^{3+} ion has a much smaller radius than La^{3+}; therefore, the replacement of the Gd^{3+} for the La^{3+} ion has the similar effect like a pressure applied to some extent. It naturally leads to an increase of Δ_{CF} and the more stabilized LS state than in the La(Sr) compounds. Indeed, very recently Knizek et al. observed a Δ_{CF} of Co ions in $GdCoO_3$ much larger than that in $LaCoO_3$.[45] The much smaller effective magnetic moment at the Co ions in the Gd(Sr) compounds relative to the La(Sr) system, suggested in Figure 5, confirms the lower spin state in the Gd(Sr) system. Furthermore, as a result of the higher acidity (i.e., a higher charge/radius ratio) of Gd^{3+}, the Gd^{3+} ions compete more strongly than La^{3+} ions with cobalt ions in covalent bonding to the oxygen atoms. This leads to narrower Co−O bands and more stable π^*(Co−O) levels.[54] This also causes a more stable LS configuration in Gd(Sr) compounds. Therefore, the smaller ion radius and the higher acidity of the Gd^{3+} ion relative to that of the La^{3+} ion lead to a larger Δ_{CF}, which favors a LS Co^{III}. The stabilized LS Co ions results in the reduction of the population of e_g electrons. This is another important cause for the less conductance and lower T_c in $Gd_{1-x}Sr_xCoO_{3-\delta}$ relative to La(Sr) and Nd(Sr) compounds.

Finally, the large magnetic moment of Gd^{3+} ($S = 7/2$, $\mu_{eff} = 7.94\ \mu_B$) should be considered. In this paper, no obvious effect of the magnetic moment of Gd^{3+} on magnetic and transport behavior is observed except for a strong paramagnetic signal in low temperatures. Nevertheless, a larger effective field than the applied field on the Co ions system can be achieved because of the easy orientation of the Gd^{3+} sublattice in a magnetic field. Rey-Cabezudo et al.[41] pointed out that the paramagnetic Gd^{3+} sublattice polarizes the cobalt magnetic clusters. It has been considered as one possible reason for the low-temperature MR. However, it has been reported that large negative MR (more than 80% at 5 K for $x = 0.09$) was observed in low temperatures for insulator-like compositions of $La_{1-x}Sr_xCoO_3$.[27] Considering the fact of the nonmagnetic La^{3+} ion, the interpretation proposed by Rey-Cabezudo et al. based on Gd^{3+} ions may be in doubt. Wu and Leighton[27] interpreted such a negative MR at low temperature in terms of a short-range FM ordered cluster model. The Co^{III} and Co^{IV} in the hole-rich clusters are aligned by the magnetic field so that an increase in the electron hopping possibility results in a negative MR. Therefore, the smallest MR observed in most metallic compositions $x = 0.45$ can be understood with the picture proposed by Wu and Leighton in the La(Sr) system. It should be pointed out that such low-temperature smallest MR in the most conductive samples is also observed in La(Sr) system.[27] This indicates that the large negative in the low temperature in Gd(Sr) compounds has the same origin as that in La(Sr) compounds.

V. Conclusion

The evolution of magnetic and transport properties with x in $Gd_{1-x}Sr_xCoO_{3-\delta}$ ($0.10 \leq x \leq 0.70$) annealed under the oxygen pressure of 165 atm at 500 °C has been systematically investigated. Cluster-glass behavior is observed in the low doping range, while the samples show the FM transition in the high doping region. The samples show insulator-like behavior for $x \leq 0.30$, and an IM transition occurs around $x = 0.35$. The optimal doping is $x = 0.45$. A striking feature is a re-entrance of insulator-like behavior in the samples with $x \geq 0.60$, arising form the large oxygen deficiency in the samples. The annealing procedure under higher oxygen pressure at higher temperature can restore the metallic state. Relative to the La(Sr) and Nd(Sr) compounds, the $Gd_{1-x}Sr_xCoO_{3-\delta}$ system exhibits less conduction and lower T_c, which can be attributed to the large global and local structural distortion and the more stable LS state of Co ions arising from the small radius of the Gd^{3+} ion.

Acknowledgment. This work is supported by the grants from the Nature Science Foundation of China and by the Ministry of Science and Technology of China, and the Knowledge Innovation Project of Chinese Academy of Sciences.

CM0521471

---

(54) Goodenough, J. B. *Prog. Solid State Chem.* **1971**, *5*, 145.